# COMBINING MESH, VOLUME, AND STREAMLINE REPRESENTATIONS FOR POLYP DETECTION IN CT COLONOGRAPHY

*V.F. van Ravesteijn[1], L. Zhao[2], C.P. Botha[2], F.H. Post[2], F.M. Vos[1,3], and L.J. van Vliet[1]*

[1]Quantitative Imaging Group, Faculty of Applied Sciences,
[2]Computer Graphics & CAD/CAM Group, Faculty of EEMCS,
Delft University of Technology, The Netherlands,
[3]Academic Medical Center, Amsterdam, The Netherlands

## ABSTRACT

CT colonography is a screening technique for adenomatous colorectal polyps, which are important precursors to colon cancer. Computer aided detection (CAD) systems are developed to assist radiologists. We present a CAD system that substantially reduces false positives while keeping the sensitivity high. Hereto, we combine protrusion measures derived from the solution of a non-linear partial differential equation (PDE) applied to both an explicit mesh and an implicit volumetric representation of the colon wall. The shape of the protruding elements is efficiently described via a technique from data visualization based on curvature streamlines. A low-complex pattern recognition system based on an intuitive feature from the aforementioned representations improves performance to less than 1.6 false positives per scan at 92% sensitivity per polyp.

## 1. INTRODUCTION

Colorectal cancer is the second leading cause of death due to cancer in the Western world [1]. It has been shown that screening for adenomatous colorectal polyps, which are important precursors to cancer, and subsequent removal of identified lesions significantly reduces the incidence of colon carcinoma [2, 3]. Computed tomography colonography (CTC) is a rapidly evolving technique that is advocated for screening. To assist the radiologists, effort is put in the development of computer aided detection (CAD) systems [4, 5, 6, 7, 8, 9].

Traditionally, polyps are tentatively detected by curvature derived features. Subsequently, the candidates thus obtained are classified features describing the image structure such as curvature and intensity. The latter are typically involved to reject falsely detected stool (frequently having a granulated grey-value structure due to air bubbles) and false detections emanating from partial volume effects. It was demonstrated that no other features but the aforementioned ones are required for a performance that is comparable to optical colonoscopy [8].

Many different approaches for polyp detection have been presented in literature. To explore whether different techniques are complementary, we revisit some techniques originated in our previous work. It has been shown that polyps can be detected equally well as protrusions on an explicit (mesh-surface) representation as on an implicit (grey-level) representation of the colon wall [9]. In this paper, we present a low-complex, unambiguous pattern recognition step, which combines the two approaches and reveals that they are to some extent complementary. Moreover, a streamline analysis, originally used in the field of data visualization, is incorporated in our framework. It will be shown that this analysis will also significantly improve the overall results.

## 2. MATERIALS

For evaluation, a subset of 28 patients from a larger study [10] is used. All patients adhered to an extensive laxative regime and no fecal tagging agent was administered. The data sets consist of scans in both prone and supine positions; the slice thickness was 3.2 mm. The reference standard is optical colonoscopy. Expert radiologists retrospectively indicated the location of polyps by annotating a point in the 3D data set using the reference standard. 65 polyp annotations were made in the 56 scans, corresponding to 40 polyps larger than or equal to 6 mm. The candidate segmentations were labeled by comparison to these annotations. A polyp was counted as a true positive CAD detection if it was found in at least one of the two scans.

## 3. PROTRUSION-BASED DETECTION OF POLYPS

Polyps may be characterized by the condition that the smallest principal curvature is larger than zero. In other words, they are caplike structures, whereas colonic folds are elongated with typically one positive curvature and the other close to zero or (slightly) negative. Because of the cylindrical global nature of the colon, regions with two positive curvatures are relatively scarce. The principal curvatures of the colon wall

can either be computed by differentiation of a mesh representation or directly from the underlying image data [11].

Previously, we introduced two distinct, iterative schemes for the detection of polypoid objects by the amount of protrusion compared to the background. The updating function in both schemes is abstractly defined as:

$$X^{t+1} = X^t + dt \cdot f(-\kappa_2) \quad (1)$$

in which $f(-\kappa_2)$ is a function that is designed to operate on an object only if the smallest curvature is positive and $dt$ is a time step [12, 9]. In the explicit method $f(\cdot)$ is related to the force applied to the mesh vertices, whereas in the implicit method this function modifies the intensity of voxels in such a way that 'protruding' intensities are smoothed into the background. Both approaches involve a repeated application of (1) until $\kappa_2$ is smaller than or equal to zero everywhere or until some convergence criterium is satisfied.

### 3.1. Complementary Protrusion Analysis

It may be concluded from the previous section that polyps are protrusions in both the explicit (mesh) and in the implicit (grey-value) representation of the colon wall. In practice we have found that particularly the false detections of both methods are to some extent uncorrelated. For instance, the explicit method typically had some false detections emanating from partial volume effects (PVE), whereas the implicit method was more robust because it took the internal intensities into account. Reversely, the implicit method, using neighbourhood information, is inherently sensitive to neighbouring structures, whereas such problems are excluded in the explicit method in which feature measurement is confined along the (infinitesimal thin) mesh. Because of the thinness of some folds, the intensities inside folds are influenced by the PVE. As a consequence, the implicit method also detects candidates inside a fold. The mesh method has only limited response at these locations.

The explicit approach directly acts on a representation of the colon wall, whereas the implicit method interacts with the underlying data. These two representations also reflect the features to distinguish true polyps from false detections. Note that the protruding aspect is predominantly represented in the mesh representing the colon wall, whereas the material structure is captured in the underlying data. We conceive a combined approach in which the protrusion extent is better represented in the explicit method, whereas the volumetric and intensity properties are delivered by the implicit method.

### 3.2. Shape Analysis

It may be observed that so far information about the shape of the objects remains limited. Effectively, lesions are detected by the amount of protrusion only, irrespective of shape. An effective representation of shape was recently described in the literature on data visualization, deriving from curvature streamline analysis.

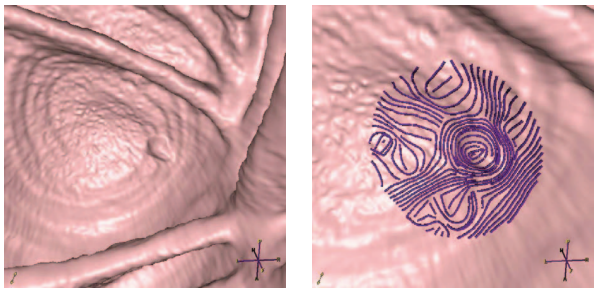

(a) (b)

**Fig. 1**: (a) A polyp with its surrounding environment. (b) Example of the curvature streamlines generated in the vicinity of the polyp.

Curvature streamlines (or lines of curvature) are defined as lines that are tangent everywhere to one of the two principal curvature direction vector fields on the surface. Techniques for deriving curvature streamlines on the surface were presented in [13]. In order to capture the essential surface shape information, streamlines were adaptively spaced over the whole surface with spacing dependent on the local principal curvature magnitudes. On less curved surface regions, fewer streamlines were generated than on highly curved surface regions.

Curvature streamlines that are constrained to the colonic wall have the useful characteristic that they tend to encircle polyp necks. The 'winding angle' feature was derived to utilize this characteristic. It is defined as the cumulative signed change of direction along a streamline. At each sample point, the differential change of direction is determined based on the surface normal at that point. Closed streamlines, such as those around polyp necks, have a winding angle of at least $2\pi$. A candidate was assigned the maximum winding angle of a streamline in its vicinity. Initial experimentation showed that this winding angle feature correlated highly with true polyp detections and could thus be useful to reduce the number of false positives (FPs) found by CAD systems [13]. Special care should be taken to ensure that streamlines are sufficiently long in order to fully capture polyp surface geometry [14].

## 4. EXPERIMENTS AND RESULTS

The detections on the explicit representation (Section 4.1) are at the basis to analyse how protrusions are detected with the implicit method and how the streamline analysis may contribute (Section 4.2). In the last section, FROC analysis shows the improvement of each newly added feature.

### 4.1. Combined CAD System Based on Protrusion

The explicit method actually involves two features. First, we use a feature derived from the displacement field of the mesh. This feature measures the percentage of the candidate with a displacement larger than a certain threshold $T$, further denoted as $\Phi_T$. We use a threshold of 0.6 mm as in [8]. This design favors candidates with steep edges and compact forms. The second feature we use is the mean intensity of the candidate [8], calculated as a tonal weighted sum of all voxels included in a segmentation mask. The latter consists of the area included between the original and the displaced mesh.

To analyse the performance of a combined system, the correspondences between candidates found by both methods should be established. The implicit method acts only on these regions in the image where a candidate was found by the explicit method. These regions are obtained by ten times dilation of the binary segmentation mask of the candidate. A corresponding segmentation area for the implicit method is derived from the deformed image by thresholding the intensity difference at a value of 100 Hounsfield unit (HU) (as in [9]). Thus, each candidate from the implicit method is inherently linked to a corresponding detection on the mesh.

Fig. 2 contains two scatter plots of the maximum intensity difference derived from the implicit method versus the maximum displacement of the mesh (Fig. 2(a)) and versus $\Phi_T$ derived from the displacement field (Fig. 2(b)). It can be seen that the maximum mesh displacement and the maximum intensity difference correlate well for polyps (black dots). In both scatter plots two regions of false detections (grey dots) can be observed in which the depicted features are uncorrelated (top-left and bottom right, dash-dotted). One region has rather low maximum intensity change but concurrently quite large maximum displacement of the mesh or $\Phi_T$; another region is characterized by a large maximum intensity difference, but a low maximum mesh displacement or $\Phi_T$. The indicated boundaries of the feature space (dashed lines) in Fig. 2(a) represent the two thresholds used in the candidate generation.

### 4.2. Streamline Analysis

For all detections on the mesh, a centerline through the center of gravity and the center of curvature of the segmentation mask is computed [15]. The intersection of this line and the mesh defines the initial seed point for the streamline analysis. For each detection curvature streamlines are generated within a spherical ROI with 16 mm radius around the seed point. As explained in Section 3.2, the winding angle is calculated on these streamlines as the cumulative signed change of direction along the streamline. At each sample point, the differential curvature is derived relative to the surface normal at that point. In other words, when a streamline forms a circle, its absolute winding angle is $2\pi$ or more (for polyp characterization the sign of the winding angle is not important). Importantly, an absolute winding angle of more than $2\pi$ is not necessarily more 'polyp-like' than a winding angle equal to $2\pi$. Therefore, we clip this feature to a maximum of $2\pi$, i.e. $\Psi_c = \min(|\Psi|, 2\pi)$. This hypothesis is confirmed by FROC analysis as shown in Fig. 4(b).

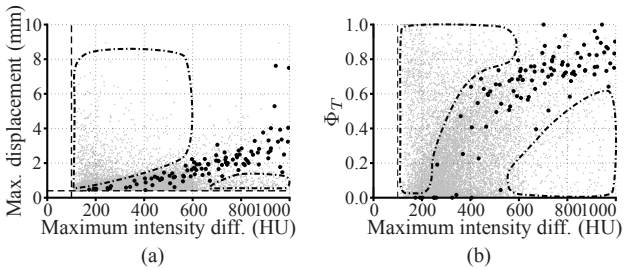


**Fig. 2**: Scatter plots of a larger (equivalent) data set (86 patients) showing (a) the maximum mesh displacement of a candidate, and (b) $\Phi_T$ vs. the maximum intensity difference derived from the implicit method. The black dots correspond to polyps and the grey dots to false detections.

Fig. 3 shows scatter plots of (a) the absolute winding angle $|\Psi|$ and (b) the clipped winding angle $\Psi_c$ vs. $\Phi_T$ (derived from the mesh displacement field). Again, the black dots denote the polyps and the grey dots denote the false detections. Observe that almost all polyps have a winding angle close to or larger than $2\pi$, whereas many false detections have lower winding angles. In other words, the winding angle might indeed help to distinguish between polyps and false detections.

### 4.3. FROC Analysis

Fig. 4 shows FROC curves describing the performance of the CAD system. The FROC curves are computed by ten times repeated ten-fold cross-validation. In all cases, we used a logistic classifier and we discarded detections on the rectal tube.

Initially, the system was based on two features: $\Phi_T$ and the mean intensity. The performance of this system (Ex) is shown in Fig. 4(a) by the dash-dotted line. Then, the implicit

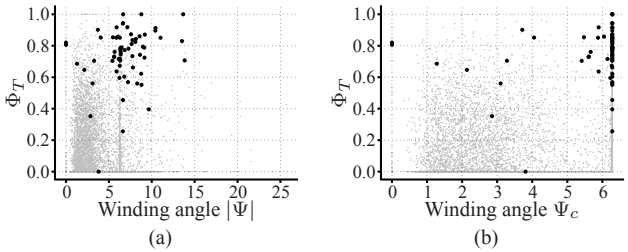


**Fig. 3**: Scatter plots showing $\Phi_T$ versus (a) $|\Psi|$ and (b) $\Psi_c$. The black dots correspond to polyps and the grey dots to false detections.

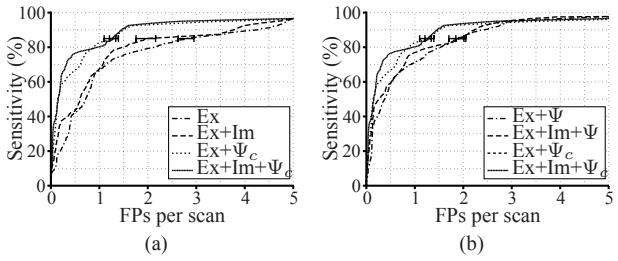


**Fig. 4**: FROC curves for polyp detection systems consisting of a combination of the explicit method (Ex), the implicit method (Im), and the streamline analysis ($\Psi/\Psi_c$).

method (Im) was added by means of the maximum intensity difference feature; the resulting performance is given by the large dashed line. Finally, the clipped winding angle feature $\Psi_c$ was included to both previous configurations, represented by the small dashed respectively the solid line. We conclude that 92% of the polyps were detected with less than 1.6 false positives per scan when all four features are included. The error bars denote two times the standard deviation in the number of false positives over all scans at 85% sensitivity. Actually, the standard deviation of the FROC curves is over seven times smaller due to averaging over all scans.

## 5. CONCLUSIONS

We present a polyp CAD system that detects polyps based on four intuitive features. The detection consists of solving Equation 1 by means of two different approaches, which characterize different aspects of the candidates. In effect, protruding objects are detected by means of deforming an explicit representation of the colon surface or by means of modifying the intensity data containing an implicit representation. We also added a shape-descriptor derived from curvature streamline analysis. It was shown that the feature based on the mesh displacement field, the mean intensity, the maximum intensity difference and the streamline's winding angle are sufficient for optimal performance. We analyzed 56 scans from 28 patients and it was found that over 92% of the polyps were detected with less than 1.6 false positives per scan.

**Acknowledgements.**

This work is supported by Philips Healthcare, Best, the Netherlands. We thank the Academic Medical Center, Amsterdam, The Netherlands for providing the data sets.

## 6. REFERENCES

[1] "Colorectal cancer facts & figures," American Cancer Society, Atlanta, Tech. Rep. No. 8617.00, 2005.

[2] J. T. Ferrucci, "Colon cancer screening with virtual colonoscopy: Promise, polyps, politics," *American Journal of Roentgenology*, vol. 177, pp. 975–988, 2001.

[3] S. Winawer, R. Fletcher *et al.*, "Colorectal cancer screening and surveillance: Clinical guidelines and rationale – update based on new evidence," *Gastroenterology*, vol. 124, pp. 544–560, 2003.

[4] A. Jerebko, S. Lakare *et al.*, "Symmetric curvature patterns for colonic polyp detection," in *Proc. MICCAI'06*, vol. LNCS 4191, 2006, pp. 169–176.

[5] G. Kiss, S. Drisis *et al.*, "Computer-aided detection of colonic polyps using low-dose CT acquisitions," *Acad Radiol*, vol. 13, no. 9, pp. 1062–1071, 2006.

[6] J. Näppi and H. Yoshida, "Fully automated three-dimensional detection of polyps in fecal-tagging CTC," *Acad Radiol*, vol. 14, pp. 287–300, 2007.

[7] R. M. Summers, J. Yao *et al.*, "Computed tomographic virtual colonoscopy computer-aided polyp detection in a screening population," *Gastroenterology*, vol. 129, pp. 1832–1844, 2005.

[8] V. F. van Ravesteijn, C. van Wijk *et al.*, "Computer aided detection of polyps in CT colonography using logistic regression," *submitted*.

[9] C. van Wijk, V. F. van Ravesteijn *et al.*, "Detection and segmentation of colonic polyps on implicit isosurfaces by second principal curvature flow," *submitted*.

[10] R. E. van Gelder, C. Y. Nio *et al.*, "Computed tomographic colonography compared with colonoscopy in patients at increased risk for colorectal cancer." *Gastroenterology*, vol. 127, no. 1, pp. 41–8, 2004.

[11] L. J. van Vliet and P. Verbeek, "Curvature and bending energy in digitized 2D and 3D images," in *Proc. 8th Scand. Conf. on Image Analysis*, 1993, pp. 1403–1410.

[12] C. van Wijk, V. F. van Ravesteijn *et al.*, "Detection of protrusions in curved folded surfaces applied to automated polyp detection in CT colonography," in *Proc. MICCAI'06*, vol. LNCS 4191, 2006, pp. 471–478.

[13] L. Zhao, C. P. Botha *et al.*, "Lines of curvature for polyp detection in virtual colonoscopy," *IEEE Trans. Vis. Comput. Graphics*, vol. 12, no. 5, pp. 885–892, 2006.

[14] ——, "Efficient seeding and defragmentation of curvature streamlines for colonic polyp detection," in *Proc. SPIE Medical Imaging 2008*, vol. 6916, no. 13, 2008.

[15] J. J. Dijkers, C. van Wijk *et al.*, "Segmentation and size measurement of polyps in CT colonography," in *Proc. MICCAI'05*, vol. LNCS 3749, 2005, pp. 712–719.